Linear Phase VDF Design with Unabridged Bandwidth Control over the Nyquist Band

S. J. Darak*, *Student Member, IEEE*, A. P. Vinod, *Senior Member, IEEE,* E. M-K. Lai, *Senior Member, IEEE,* J. Palicot, *Senior Member*, *IEEE*, H. Zhang, *Senior Member, IEEE*

***Abstract*— This brief presents a low complexity linear phase variable digital filter (VDF) design with tunable lowpass (LP), highpass (HP), bandpass (BP) and bandstop (BS) responses anywhere over entire Nyquist band. The spectral parameter approximation based VDFs (SPA-VDFs) designed using Farrow structure have advantages of linear phase, lower group delay and fewer variable multipliers. However, the total gate count and dynamic range of filter coefficient values of SPA-VDFs increase significantly with the tunable range of cut-off frequency which limits their usefulness in emerging signal processing and wireless communication applications. Also, existing VDFs need to update either filter coefficients or need parallel filter structures to obtain variable LP, HP, BP and BS responses. In this paper, a new VDF design is proposed by deftly integrating SPA-VDF with the modified coefficient decimation method (MCDM) and it shall be referred to as SPA-MCDM-VDF. The SPA-MCDM-VDF provides LP, HP, BP and BS responses with unabridged center frequency and bandwidth control over the entire Nyquist band without the need for hardware re-implementation or coefficient update. The complexity comparisons show that the SPA-MCDM-VDF offers substantial savings in gate count, group delay and number of variable multiplications over other linear phase VDFs.**

***Index Terms*—modified coefficient decimation method, spectral parameter approximation, variable digital filter.**

I. Introduction

Variable digital filters (VDFs) are digital filters with adjustable cut-off frequencies that are controlled through a small number of parameters. VDFs are useful in applications such as channelization in software defined radios, spectrum sensing in emerging cognitive radios, adaptive systems, biomedical applications [1-13] and reconfigurable filter bank design [14-15]. For such applications, the VDF must be able to produce tunable lowpass (LP), highpass (HP), bandpass (BP) and bandstop (BS) responses without hardware re-implementation or coefficient update. Moreover, the VDF should be hardware-efficient in terms of area, power and delay. Realizing such linear phase VDFs is a challenging task.

A number of linear and non-linear phase VDF designs are available [1-14]. The allpass transformation (APT) based VDFs (APT-VDFs) [1] are obtained by replacing each unit delay of a digital filter by an APT structure of an appropriate order and they allow on-the-fly control over the cut-off frequency. A low complexity APT-VDF in [2] provides variable LP, HP, BP and BS responses from a fixed-coefficient prototype filter. However, because of non-linear phase characteristics, APT-VDFs are not preferred for many signal processing and wireless communication applications. In [3], a frequency transformation based linear phase VDF is proposed and it is further extended in [4, 5]. The modified frequency transformation based VDF (MFT-VDF) [6] provides variable LP, HP, BP and BS responses from a fixed-coefficient prototype filter but only over limited section of Nyquist band. The VDFs in [12, 13] offer wide cut-off frequency range with sharp transition bandwidth (TBW) but the group delay is huge.

Spectral parameter approximation based VDFs (SPA-VDFs) [7-12] are designed using the Farrow structure. Their advantages over other VDFs [1-6] include fixed TBW, lower group delay, fewer variable multiplications (VMs) and high accuracy. Also, multiple responses can be easily obtained using SPA-VDFs than other VDFs [1-6, 12, 13]. However, the total gate count requirement of SPA-VDFs is very high [11]. Furthermore, the coefficient values of the sub-filters in SPA-VDFs increase exponentially with their order which may impose constraints when fixed-point implementation is needed. In [11], the solution to this problem is provided by appropriate selection of range of VM. Still, the dynamic range of sub-filter coefficients is comparatively large than other VDFs especially when the tunable range of cut-off frequency is wide which limits the usefulness of SPA-VDFs for many emerging communication applications. The narrow cut-off frequency range also limits the bandwidth and center frequency range of BP and BS responses. Most of the current research on SPA-VDFs is focused on algorithms for optimizing sub-filter coefficients thereby improving the mean square error and reducing offline processing time. There is hardly any work on low complexity architectures for SPA-VDF with wide range of cut-off frequency.

In this brief, a low complexity VDF designed by deft integration of the SPA-VDF with modified coefficient decimation method (MCDM) is proposed. It shall be referred to as SPA-MCDM-VDF. The design example shows that

S. J. Darak and A.P. Vinod are with the School of Computer Engineering, Nanyang Technological University, 639798 Singapore (Email: dara0003@e.ntu.edu.sg ; asvinod@ntu.edu.sg).

E. M-K. Lai is with the School of Engineering and Advanced Technology, Massey University, Albany, New Zealand. (Email: E.Lai@massey.ac.nz).

J. Palicot and H. Zhang are with the Supélec, Rennes and Université Européenne de Bretagne, Rennes, France respectively. (Email: Jacques.palicot@supelec.fr; honggang.zhang@supelec.fr).

SPA-MCDM-VDF provides variable LP, HP, BP and BS responses with unabridged bandwidth control over the entire Nyquist band without the hardware re-implementation or coefficient update. The complexity comparison shows that the SPA-MCDM-VDF offers substantial savings in total gate count, VMs and group delay over other linear phase VDFs.

The rest of the paper is organized as follows. A brief review of SPA-VDFs and MCDM is presented in Section II. The design and architecture of the SPA-MCDM-VDF are explained in Section III. A design example and complexity comparisons are shown in Section IV and V respectively. Finally, Section VI concludes the paper.

II. SPA-VDFs and MCDM Review

A. Spectral parameter approximation based VDFs

The block diagram of a SPA-VDF, $H_\alpha(z)$, is shown in Fig. 1. The transfer function can be expressed as

$$H_\alpha(z) = \sum_{k=0}^{L} H_k(z)\, \alpha^k \tag{1}$$

where $H_k(z)$, $0 \le k \le L$, are N^{th} order fixed-coefficient linear phase sub-filters and α is the parameter which controls the cut-off frequency of the $H_\alpha(z)$ [8-11]. The transfer function of k^{th} N^{th} order sub-filter, $H_k(z)$, is given by,

$$H_k(z) = \sum_{n=0}^{N} h_k(n) z^{-n} \tag{2}$$

where $h_k(n)$ is the symmetrical impulse response of $H_k(z)$. Substituting (2) into (1), we have [10]

$$H_\alpha(z) = \sum_{k=0}^{L} \sum_{n=0}^{N} h_k(n) z^{-n}\ \alpha^k \tag{3}$$

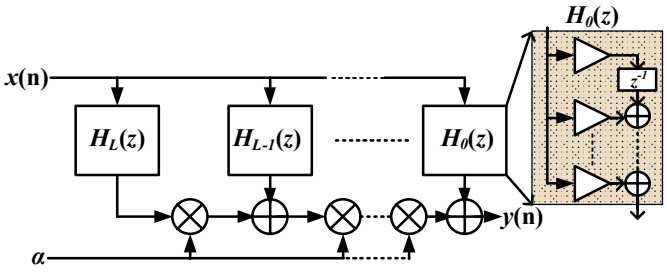

Fig. 1. SPA-VDF, $H_\alpha(z)$, with FIR sub-filters in transposed direct form.

A number of optimization techniques such as minimax approximation, linear programming, least square, weighted least square and constrained least square have been used to determine sub-filter coefficients, $h_k(n)$, so that the frequency response of $H_\alpha(z)$ will precisely approximate the desired response as a function of α [7-11]. The advantage of $H_\alpha(z)$ architecture over [1-6, 12, 13] is that multiple responses can be easily obtained by using parallel branches of VMs, α. The cut-off frequency of each response can be tuned individually. The group delay of $H_\alpha(z)$ is $N/2$ and very low.

B. Modified Coefficient Decimation Method (*MCDM*)

The modified coefficient decimation method (MCDM abbreviated as MCDM-I in literature) has been used for the design of reconfigurable filters and filter banks [14]. In MCDM using decimation factor D, every D^{th} coefficient of the prototype filter, $H(e^{j\omega})$, is retained and others are replaced by zeros. Then, the sign of every alternate retained coefficient is reversed to obtain a multi-band frequency response, $H_D^m(e^{j\omega})$, which is given by [14],

$$H_D^m(e^{j\omega}) = \frac{1}{D}\sum_{k=0}^{D-1} H\left(e^{j\left(\omega - \frac{\pi(2k+1)}{D}\right)}\right) \tag{4}$$

The $H_D^m(e^{j\omega})$ consists of multiple subbands located at multiples of (π/D) [14]. The bandwidth and the TBW of all the subbands in $H_D^m(e^{j\omega})$ are identical and equal to the bandwidth and the TBW of $H(e^{j\omega})$ respectively. However, MCDM-VDF fails to provide an unabridged bandwidth and location control over Nyquist band due to integer$D$.

III. Proposed SPA-MCDM-VDF

The goal of the proposed SPA-MCDM-VDF is to provide tunable LP, HP, BP and BS responses over entire Nyquist band without the need of time consuming hardware re-implementation or coefficient update. This is achieved by deftly integrating lowpass SPA-VDF with the MCDM. The SPA-MCDM-VDF is not just straightforward integration of these two techniques. In fact, the SPA-MCDM-VDF is carefully designed by exploiting architectural advantages of the Farrow structure as well as exclusive multiband response capability of MCDM. The design and architecture of the SPA-MCDM-VDF are explained in detail below.

A. Basic Principle

Consider the four equal parts of Nyquist band: $(0 - 0.25\pi)$, $(0.25\pi - 0.5\pi)$, $(0.5\pi - 0.75\pi)$ and $(0.75\pi - \pi)$. The basic principle of SPA-MCDM-VDF is that using LP prototype filter with cut-off frequency, ω_c, three additional LP responses with cut-off frequencies $(\pi - \omega_c)$, $(0.5\pi - \omega_c)$ and $(0.5\pi + \omega_c)$ can be obtained via MCDM. Based on this principle, the prototype filter in the MCDM is replaced with the prototype SPA-VDF, $H_\alpha(z)$, that provides variable LP responses with TBW of TBW_d and unabridged control over cut-off frequency, $\omega_{cp\alpha}$, in the second quarter i.e. $0.25\pi \le \omega_{cp\alpha} \le 0.5\pi$. Then, LP responses with ω_c in each quarter of the Nyquist band i.e. $\left\{\left(\frac{TBW_d}{2}\right)\pi \le \omega_c \le \left[1 - \left(\frac{TBW_d}{2}\right)\right]\pi\right\}$ are obtained as follows.

1) ***LP response in the second quarter*:** $H_\alpha(z)$ provides LP responses in second quarter. The frequency response of $H_\alpha(z)$ is shown in Fig. 2(a). It is also denoted by $H_{\alpha 02}^m(e^{j\omega_c})$ where subscripts '0' and '2' represents D=0 and second quarter respectively.

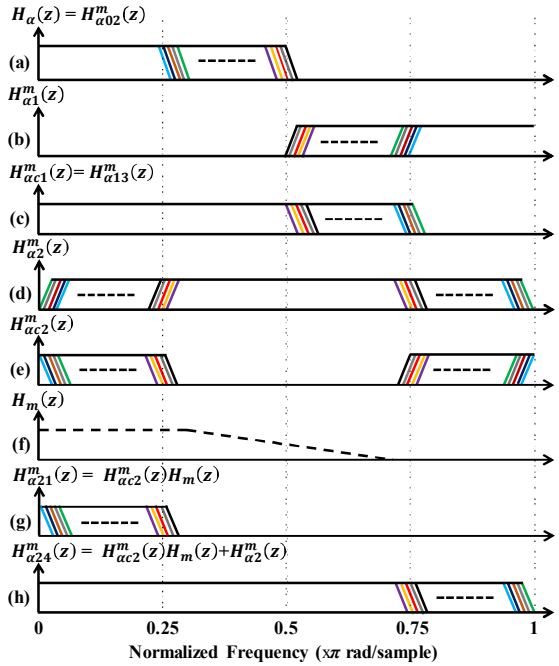

Fig. 2. (a) Frequency response of lowpass prototype VDF, $\boldsymbol{H_\alpha(z)}$, (b) Frequency response, $\boldsymbol{H^m_{\alpha1}(z)}$, (c) Complementary response, $\boldsymbol{H^m_{\alpha c1}(z)}$, of (*b*), (d) Frequency response, $\boldsymbol{H^m_{\alpha2}(z)}$, (e) Complementary response, $\boldsymbol{H^m_{\alpha c2}(z)}$, of (*d*), (f) Frequency response of masking filter, $\boldsymbol{H_m(z)}$, (g) Frequency response of $(\boldsymbol{H^m_{\alpha c2}(z)H_m(z)})$, (h) Frequency response of $(\boldsymbol{H^m_{\alpha c2}(z)H_m(z) + H^m_{\alpha2}(z)})$.

2) ***LP response in the third quarter*:** Using the MCDM with D =1, the HP responses, $H^m_{\alpha1}(z)$, with cut-off frequencies in the third quarter can be obtained as shown in Fig. 2(b). By complementing $H^m_{\alpha1}(z)$, we have the LP responses $H^m_{\alpha13}(e^{j\omega_c})$ with ω_c = (π - $\omega_{cp\alpha}$) as shown in Fig. 2(c). Mathematically, these operations can be expressed as

$$H^m_{\alpha13}(e^{j\omega_c}) = \left(e^{-j\omega_{cp\alpha}\left(\frac{N-1}{2}\right)}\right) - H_\alpha\left(e^{j(\omega_{cp\alpha}-\pi)}\right) \quad (5)$$

3) ***LP response in the first quarter*:** Using MCDM with D = 2, we have bandpass response, $H^m_{\alpha2}(z)$ and its complementary bandstop response, $H^m_{\alpha c2}(z)$ as shown in Fig. 2(d) and Fig. 2(e) respectively. The higher frequency subband of $H^m_{\alpha c2}(z)$ can be masked using N^{th}_m order masking filter, $H_m(z)$, shown in Fig. 2(f). This results in LP responses, $H^m_{\alpha21}(e^{j\omega_c})$, with ω_c = (0.5*π - $\omega_{cp\alpha}$) i.e. $\left(\frac{TBW_d}{2}\right)\pi \le \omega_c \le 0.25\pi$ as shown in Fig. 2(g). Mathematically,

$$H^m_{\alpha21}(e^{j\omega_c}) = H^m_{\alpha c2}(e^{j\omega_c})H_m(e^{j0.5\pi}) \quad (6)$$

where

$$H^m_{\alpha c2}(e^{j\omega_c}) = \left\{\left(e^{-j\omega_{cp\alpha}\left(\frac{N-1}{2}\right)}\right) - \left[\frac{1}{2}\sum_{k=0}^{1} H_\alpha\left(e^{j\left(\omega_{cp\alpha}-\frac{\pi(2k+1)}{2}\right)}\right)\right]\right\}$$

4) ***LP Response in the fourth quarter*:** Adding the response $H^m_{\alpha2}(z)$ to $H^m_{\alpha21}(z)$, the LP responses with ω_c = (0.5*π + $\omega_{cp\alpha}$) i.e. $0.75\pi \le \omega_c \le \left[1 - \left(\frac{TBW_d}{2}\right)\right]\pi$, can be obtained as shown in Fig. 2(h). Mathematically,

$$H^m_{\alpha24}(e^{j\omega_c}) = H^m_{\alpha21}(e^{j\omega_c}) + H^m_{\alpha2}(e^{j\omega_c})\left[e^{-j\omega_{cp\alpha}\left(\frac{N_m-1}{2}\right)}\right] \quad (7)$$

where

$$H^m_{\alpha2}(e^{j\omega_c}) = \left\{\left[\frac{1}{2}\sum_{k=0}^{1} H_\alpha\left(e^{j\left(\omega_{cp\alpha}-\frac{\pi(2k+1)}{2}\right)}\right)\right]\right\}$$

The HP responses can be obtained by complementing corresponding LP responses. Furthermore, the BP responses with lower and upper cut-off frequencies of ω_l and ω_h, respectively can be obtained by subtracting the LP response with ω_l from another LP response with ω_h. Likewise, the BS responses can be obtained. The TBW of all the responses is fixed and equal to TBW_d. Since the range of ω_c of LP response is $\left\{\left(\frac{TBW_d}{2}\right)\pi \le \omega_c \le \left[1 - \left(\frac{TBW_d}{2}\right)\right]\pi\right\}$ which spans entire Nyquist band, ω_l and ω_h of BP and BS responses are not restricted to limited values unlike other VDFs [1-14].

B. Architecture of the SPA-MCDM-VDF

The architecture of the SPA-MCDM-VDF is shown in Fig. 3. It consists of prototype SPA-VDF, $H_\alpha(z)$, which has (L+1) fixed-coefficient sub-filters, $H_k(z)$, $0 \le k \le L$ each of order N. Fig. 4 shows the detailed architecture of the k^{th}sub-filter. The prototype $H_\alpha(z)$ provides variable LP responses with TBW of TBW_d, $0.25\pi \le \omega_{cp\alpha} \le 0.5\pi$, passband and stopband ripple of δ_p and δ_s respectively. Here, $H_\alpha(z)$ is designed using optimization algorithm in [12] and hence ($0 \le \alpha \le 1$) but any one of the optimization algorithms in [7-11] can be used. Since the MCDM with D = 2 leads to the deterioration in stopband ripple, δ_s of $H_\alpha(z)$ should be $(\delta_{sd}/2)$ i.e. $(\delta_s)_{dB} = [(\delta_{sd})_{dB} - 6]$ where δ_{sd} is the desired stopband ripple of the SPA-MCDM-VDF.

In Fig. 3, control signals, *sel1_D* and *sel2_D*, select the MCDM factor D for the two branches of these sub-filters [14]. The details of MCDM implementation are given in [14]. The fixed-coefficient masking filter, $H_m(z)$, of order N_m with cut-off frequency and TBW of 0.5 and (0.5 – 2*TBW_d), respectively is used to mask the higher frequency subband of $H^m_{\alpha c2}(z)$ as discussed Section III.A. The sub-filters along with controlling parameter, α_1 provide LP response, $y_{LP}(z)$, using one of the steps 1-4 described in Section III.A. The numbers at the input of a multiplexer of $y_{LP}(z)$ indicate the quarter of Nyquist band they belong. The control signals of all multiplexers are combined and named as *sel* which is 10 bit wide. For example, 7th and 8th bits of *sel* are given to 4:1 multiplexer numbered 5 and so on. In case of LP response, branch with α_2 is not used. Then, the *sel* signal to obtain LP response in quarter 1, 2, 3 and 4 is 'x0xxxxxx11', 'xxxxxxxx00', 'xxxxxxxx01' and 'x0xxxxxx10' respectively. In case of BP response, $y_{BP}(z)$, *sel* signal depends on the quarters to which ω_l and ω_h belong and are given in Table I. Here, 'x' denotes don't care and third column indicates the cut-off frequency (either ω_l or ω_h) of LP response produced by the branch with α_1. Then, the branch with α_2 produce LP response with remaining cut-off frequency.

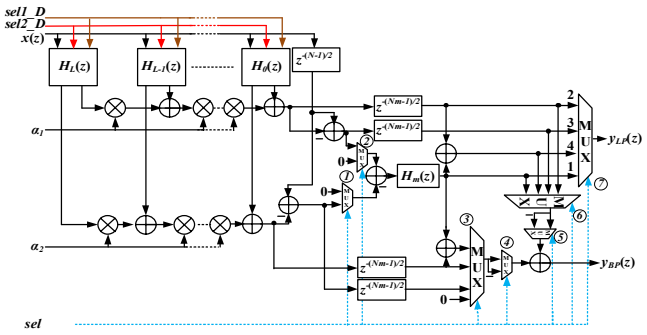

Fig. 3. Architecture of the SPA-MCDM-VDF.

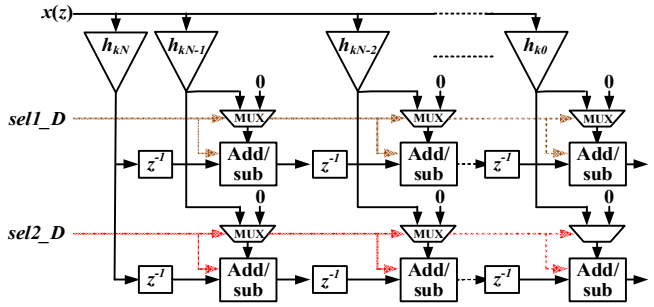

Fig. 4. Architecture of sub-filter, $H_k(z)$.

TABLE I. MULTIPLEXER'S SETTINGS FOR BANDPASS RESPONSES.

ω_l	ω_h	α_1	*sel*
1	1	ω_h	10110011XX
1	2	ω_l	00010111XX
1	3	ω_l	00100111XX
1	4	$\max(\omega_l, \pi - \omega_h)$	10110010XX
2	2,3,4	ω_h	{0X011000XX}, {0X011001XX}, {00011010XX}
3	3,4	ω_h	{0X101001XX}, {00101010XX}
4	4	ω_l	10010110XX

IV. DESIGN EXAMPLE

Consider the first design example with $TBW_d = 0.2\pi$, δ_{sd} = -50 dB and δ_{pd} = 0.1 dB. Then, the range of ω_c is 0.1π to 0.9π. For these specifications, the SPA-MCDM-VDF is designed with L=5, N=32, N_m=18 and corresponding variable LP responses are shown in Fig. 5 where responses in blue, green, red and black colors are the those obtained using the respective steps 1-4 in Section III.A. The BP responses are shown in Fig. 6 (for fixed center frequency) and Fig. 7 (for variable center frequency) which show unabridged and independent control over both the lower and upper cut-off frequencies. For second design example with $TBW_d = 0.08\pi$, δ_{sd} = -40 dB, δ_{pd} = 0.5 dB and hence, $0.04\pi \le \omega_c \le 0.96\pi$, SPA-MCDM-VDF is designed with L=10, N=80, N_m=14. Corresponding LP responses are shown in Fig. 8.

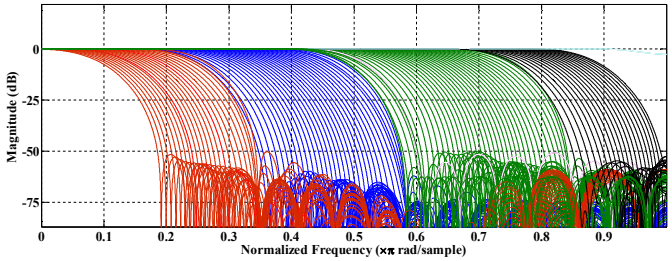

Fig. 5. Variable LP responses using the SPA-MCDM-VDF ($TBW_d = 0.2\pi$).

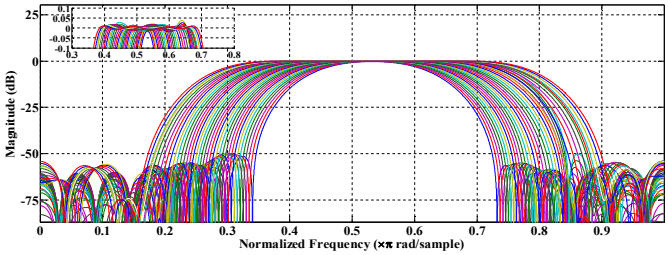

Fig. 6. Variable BP responses using the SPA-MCDM-VDF ($TBW_d = 0.2\pi$).

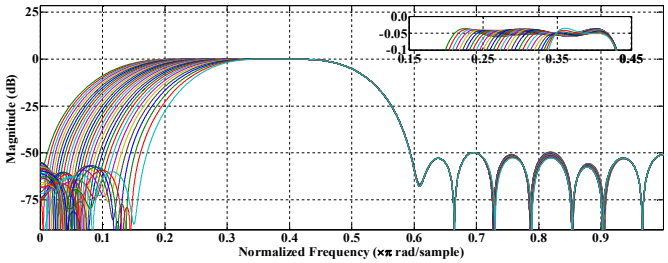

Fig. 7. Variable center frequency BP responses using the SPA-MCDM-VDF ($TBW_d = 0.2\pi$).

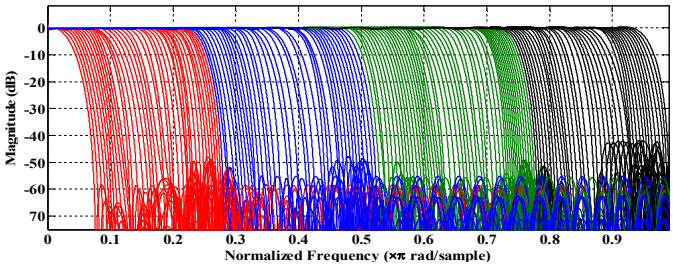

Fig. 8. Variable LP responses using the SPA-MCDM-VDF ($TBW_d = 0.08\pi$).

V. COMPLEXITY COMPARISON

A 16x16 bit multiplier, a 2:1 multiplexer, a 4:1 multiplexer and 32 bit adder were synthesized on a TSMC 0.18µm process. The Synopsys Design Compiler was used to estimate the cell area. The gate count is obtained by normalizing the cell area values by that of a 2:1 NAND gate from the same library. The total gate count in Table II is the sum of the gate counts of all the components and NA means not applicable.

For the first design example discussed in Section IV, SPA-VDF [10] consists of 16 sub-filters each of order 62. The SPA-VDF in [11] consists of two sets of sub-filters to obtain LP responses in first and second quarters. Each set consists of 5 sub-filters of order 32. To obtain BP and BS response, SPA-VDFs [10, 11] need two branches of VMs. Since the MCDM-VDF [14] provides only coarse control over the cut-off frequency, the resolution between cut-off frequencies is fixed at 0.02π. In this case, the order of the prototype filter is 1000 and the range of D is 1 to 25. The order of the prototype filter in MFT-VDF [6] and APT-VDF [2] is 40 and 48 respectively.

The SPA-MCDM-VDF requires 73%, 17.5%, 78% and 10% lower gate count than that of SPA-VDF [10], SPA-VDF in [11], MCDM-VDF [14] and MFT-VDF [6] respectively for the first design example. Similar savings are also achieved in case of second design example as shown in Table II. The group delay of the SPA-MCDM-VDF is very low. Though the gate count of non-linear phase APT-VDF is low, the SPA-

TABLE II. GATE-COUNT COMPLEXITY COMPARISON.

No. of VDFs	$TBW_d = 0.2\pi$, δ_{sd} = -50 dB, δ_{pd} = 0.1 dB					$TBW_d = 0.08\pi$, δ_{sd} = -40 dB, δ_{pd} = 0.5 dB		
	Multipliers	**MUX**	**Adders**	**Total gate count**	**Group Delay**	**Multipliers**	**Total gate count**	**Group Delay**
SPA-VDF [10]	542 (VM: 30)	0	1023	**1097375**	**31**	1874 (VM: 54)	**3817175**	**64**
SPA-VDF [11]	178 (VM: 8)	8	331	**359475**	**16**	756 (VM: 16)	**1535125**	**40**
MCDM-VDF [14]	503 (VM: 0)	2000	2001	**1325025**	**≤ 500**	1103 (VM: 0)	**2909025**	**≤ 1100**
MFT-VDF [6]	163 (VM:80)	43	301	**330030**	**80**	583 (VM: 290)	**1182893**	**290**
APT-VDF [2]	73 (VM:48)	144	144	**154240**	**NA**	331 (VM:220)	**701200**	**NA**
SPA-MCDM-VDF	122 (VM:10)	216	417	**296585**	**25**	436 (VM: 18)	**1095045**	**47**

MCDM-VDF is suitable for many signal processing and communication applications due to linear phase property.

The gate counts in Table II does not take into account the fact that the implementation complexity of VM is more than double than that of fixed multiplication (FM) [11]. It can be observed that the SPA-MCDM-VDF requires fewer VMs than VDFs in [2, 6, 10] and this difference in VMs increases as TBW_d decreases especially in case of [6] and [2]. This means that the SPA-MCDM-VDF will offer further savings in implementation complexity over [6]. In case of [2], number of VMs are 48 and 220 compared to 10 and 18 in the SPA-MCDM-VDF for design example 1 and 2 respectively. Without loss of generality, it can be inferred that the implementation complexity of SPA-MCDM-VDF will be equal to or even less than that of [2]. Furthermore, to obtain addition response, SPA-MCDM-VDF requires only 14 extra multipliers compared to 80 in [6] and 48 in [2].

The VDF in [13] employs fast filter bank approach to obtain LP responses with sharp TBW_d over wide cut-off frequency range. For new design example with sharp $TBW_d = 0.01\pi$ and $0.005\pi \leq \omega_c \leq 0.995\pi$, the VDF in [13] requires 51% lower gate count than SPA-MCDM-VDF. However, group delay of SPA-MCDM-VDF is only 294 compared to 2450 in case of [13]. Though SPA-MCDM-VDF and [13] exhibit transients, the transients in SPA-MCDM-VDF are very small due to lower order of masking filter compared to [13]. Also, SPA-MCDM-VDF has the advantages of simple architecture, fewer VMs and easy to design over [13].

VI. CONCLUSION

In this paper, a low complexity linear phase variable digital filter (VDF) by integrating spectral parameter approximation based VDF (SPA-VDF) with modified coefficient decimation method (MCDM) is presented and it is termed as SPA-MCDM-VDF. The SPA-MCDM-VDF overcomes the drawback of narrow cut-off frequency range in existing VDFs without compromising on total gate counts, group delay and dynamic range of filter coefficient values. The design examples demonstrated that SPA-MCDM-VDF provides variable lowpass, highpass, bandpass and bandstop responses with unabridged and independent control over the cut-off frequencies on the entire Nyquist band. The SPA-MCDM-VDF provides substantial savings in gate count and group delay over other linear phase VDFs.

The simple architecture, ease of design, fewer variable multipliers and ability to provide multiple responses makes SPA-MCDM-VDF suitable for design of variable resolution filter bank with independent and individual control over subband bandwidths as well as their locations. The future work will explore the design of such filter banks and its efficient implementation in FPGA via partial reconfiguration.

REFERENCES

[1] A. G. Constantinides, "Spectral transformations for digital filters," in *Proceedings of the Institution of Electrical Engineers*, vol. 117, no. 8, pp. 1585-1590, Aug. 1970.

[2] S. J. Darak, A. P. Vinod and E. M-K. Lai, "Efficient implementation of reconfigurable warped digital filters with variable lowpass, highpass, bandpass and bandstop responses," *IEEE Transactions on Very Large Scale Integration Systems*, vol. 21, no. 6, pp. 1165-1169, June 2013.

[3] A. Oppenheim, W. Mechlenbräuker, and R. Mersereau, "Variable cutoff linear phase digital filters," *IEEE Transactions Circuits and Systems*, vol. 23, no. 4, pp. 199–203, Apr. 1976.

[4] S. Hazra, "Linear phase bandpass digital filters with variable cutoff frequencies," *IEEE Transactions on Circuits and Systems*, vol. 31, no. 7, pp. 661-663, July 1984.

[5] S. D. Roy and S. Ahuja, "Frequency transformations for linear-phase variable-cutoff digital filters," *IEEE Transactions Circuits and Systems*, vol. 26, no. 1, pp. 73–75, Jan. 1979.

[6] S. J. Darak, A. P. Vinod and E. M-K. Lai, "Design of variable linear phase FIR filters based on second order frequency transformations and coefficient decimation," *IEEE International Symposium on Circuits and Systems (ISCAS),* pp. 3182-3185, Seoul, South Korea, May 2012.

[7] T. B. Deng, "Closed form design and efficient implementation of variable digital filters with simultaneously tunable magnitude and fractional delay," *IEEE Transactions on Signal Processing*, vol. 52, no. 6, pp. 1668-1681, June 2004.

[8] H. Johansson and P. Löwenborg, "On linear-phase FIR filters with variable bandwidth," *IEEE Transactions on Circuits and Systems-II*, vol. 51, no. 4, pp. 181-184, April 2004.

[9] S. C. Chan, C. K. S. Pun, and K. L. Ho, "A new method for designing FIR filters with variable characteristics," *IEEE Signal Processing Letters*, vol. 11, no. 2, pp. 274–277, Feb. 2004.

[10] S. S. Kidambi, "An efficient closed-form approach to the design of linear-phase FIR digital filters with variable-bandwidth characteristics," *Signal Processing* (*Elsevier*), vol. 86, no. 7, pp. 1656-1669, Oct 2005.

[11] P. Löwenborg and H. Johansson, "Minimax design of adjustable bandwidth linear-phase FIR filters," *IEEE Transactions on Circuits and Systems-I*, vol. 53, no. 2, pp. 431–439, Feb. 2006.

[12] D. Harris, "Computationally efficient variable linear-phase filters," *MSc thesis*, University of Miami, Florida, USA, March 2007.

[13] Y. J. Yu, "Design of variable bandedge FIR filters with extremely large bandedge variation range," *IEEE International Symposium on Circuits and Systems* (*ISCAS*), pp. 141-144, Rio de Janeiro, Brazil, May 2011.

[14] A. Ambede, K. G. Smitha and A. P. Vinod, "A low complexity uniform and non-uniform digital filter bank based on an improved coefficient decimation method for multi-standard communication channelizers," *Circuits, Systems and Signal Processing* (*Springer*), DOI- 10.1007/s00034-012-9532-9, Dec. 2012.

[15] S. J. Darak, A. P. Vinod, K. G. Smitha and E. M-K. Lai, "A low complexity non-uniform fast filter bank for multi-standard wireless receivers," *IEEE Transactions on Very Large Scale Integration (VLSI) Systems*, accepted for publication in May 2013.